Superfluidity and collective properties of excitonic polaritons in gapped graphene in a microcavity

Oleg L. Berman,[1,2] Roman Ya. Kezerashvili,[1,2] and Klaus Ziegler[1,3]

[1]*Physics Department, New York City College of Technology, The City University of New York, Brooklyn, New York 11201, USA*

[2]*The Graduate School and University Center, The City University of New York, New York, New York 10016, USA*

[3]*Institut für Physik, Universität Augsburg, D-86135 Augsburg, Germany*

(Received 16 May 2012; revised manuscript received 10 October 2012; published 5 December 2012)

We predict the formation and superfluidity of polaritons in an optical microcavity formed by excitons in gapped graphene embedded there and microcavity photons. The Rabi splitting related to the creation of an exciton in a graphene layer in the presence of the band gap is obtained. It is demonstrated that the Rabi splitting decreases when the energy gap increases, while the larger value of the dielectric constant of the microcavity gives a smaller value for the Rabi splitting. The analysis of collective excitations as well as the sound velocity is presented. We show that the superfluid density n_s and temperature of the Kosterlitz-Thouless phase transition T_c are decreasing functions of the energy gap.

DOI: 10.1103/PhysRevB.86.235404 PACS number(s): 78.67.Wj, 71.35.Lk, 71.36.+c

I. INTRODUCTION

To date, theoretical and experimental studies have been devoted to Bose coherent effects of two-dimensional (2D) excitonic polaritons in a quantum well embedded in a semiconductor microcavity.[1–4] To obtain polaritons, two mirrors are placed opposite each other in order to form a microcavity, and quantum wells are embedded within the cavity at the antinodes of the confined optical mode. The resonant exciton-photon interaction results in the Rabi splitting of the excitation spectrum. Two polariton branches appear in the spectrum due to the resonant exciton-photon coupling. The lower polariton branch of the spectrum has a minimum at zero momentum. The effective mass of the lower polariton is extremely small. These lower polaritons form a 2D weakly interacting Bose gas. The extremely light mass of these bosonic quasiparticles at experimentally achievable excitonic densities results in a relatively high critical temperature for superfluidity. The critical temperature is relatively high because the 2D thermal de Broglie wavelength is inversely proportional to the mass of the quasiparticle, and this wavelength becomes comparable to the distance between the bosons.

Recently there have been many experimental and theoretical studies devoted to graphene, known for unusual properties in its band structure.[5,6] Due to the absence of a gap between the conduction and valence bands in graphene, the screening effects result in the absence of excitonic excitations in graphene. To date, we have achieved different ways to obtain a gap in graphene. For example, the gap in graphene structures can be formed due to a magnetic field, doping, an electric field in biased graphene, and finite size quantization in graphene nanoribbons. A gap in the electron spectrum in graphene can be opened by applying a magnetic field, which results in the formation of magnetoexcitons.[7] Excitons in graphene can be also formed due to a gap opening in the electron and hole spectra in the graphene layer by doping.[8] There have been a number of papers devoted to the excitonic effects in different graphene-based structures. Significant excitonic effects related to strong electron-hole correlations were observed in graphene by measuring its optical conductivity in a broad spectral range.[9] The observed excitonic resonance was explained within a phenomenological model as a Fano interference of a strongly coupled excitonic state and a band continuum.[9] The electron-hole pair condensation in the two graphene layers has been studied in Refs. 10–14. The possibility of formation of edge-state excitons in graphene nanoribbons is caused by the appearance of the gap in the electron energy spectrum due to the finite-size quantization. A first-principles calculation of the optical properties of armchair-edged graphene nanoribbons, taking into consideration many-electron and excitonic effects, was presented in Ref. 15. Yang *et al.*[16] studied the optical properties of zigzag-edged graphene nanoribbons with the spin interaction. It was found that optical response was dominated by magnetic edge-state-derived excitons with large binding energy. First-principles calculations of many-electron effects on the optical response of graphene, bilayer graphene, and graphite were performed in Ref. 17. It was found that resonant excitons were formed in these two-dimensional semimetals. The other mechanism of electronic excitations in graphene can be achieved in biased graphene, where the energy band gap is formed by an applied electric field. A continuously tunable band gap of up to 250 meV was generated in biased bilayer graphene.[18] It was shown that the optical response of this system is dominated by bound excitons.[19]

According to Ref. 20 a tunable gap in graphene can be induced and controlled by hydrogenation. The excitons in gapped graphene can be created by laser pumping. The superfluidity of quasi-two-dimensional dipole excitons in double-layer graphene in the presence of band gaps was proposed recently in Ref. 21.

The Bose-Einstein condensation (BEC) of magnetoexcitonic polaritons formed by magnetoexcitons in graphene embedded in a semiconductor microcavity in a high magnetic field in a planar harmonic potential trap was studied in Ref. 22. However, the superfluidity of magnetoexcitonic polaritons in graphene in this case is absent, since the superfluidity is caused by the sound spectrum of Bose collective excitations due to the exciton-exciton interaction, which is negligible in graphene in a high magnetic field, in analogy to 2D magnetoexcitons in a quantum well.[23]

In this paper we consider the direct 2D excitons formed in a single graphene layer in the presence of the band gap and predict the superfluidity of polaritons formed by these

excitons and microcavity photons, when the graphene layer is embedded into an optical microcavity. We obtained the corresponding superfluid density and temperature for the Kosterlitz-Thouless phase transition due to the superfluidity of microcavity polaritons.

The paper is organized in the following way. In Sec. II we present the Hamiltonian of excitons in a graphene layer embedded in an optical microcavity. In Sec. III we obtain the excitonic Hamiltonian, which is the sum of the Hamiltonian of noninteracting excitons in gapped graphene and the Hamiltonian that describes the exciton-exciton interaction. The Hamiltonian of photons in a semiconductor microcavity is given in Sec. IV. In Sec. V the Hamiltonian of the harmonic exciton-photon coupling in gapped graphene is derived and the corresponding Rabi splitting is obtained. The study of the condensation of a gas of microcavity polaritons, the density of the superfluid component, as well as the Kosterlitz-Thouless temperature are presented in Sec. VI. Finally, the discussion of the results and the conclusions follow in Sec. VII.

II. HAMILTONIAN OF GAPPED GRAPHENE EXCITONS IN A MICROCAVITY

The total Hamiltonian $\hat{H}_{\rm tot}$ of the system of 2D excitons in gapped graphene embedded in an optical microcavity and 2D microcavity photons can be written as

$$\hat{H}_{\rm tot} = \hat{H}_{\rm ex} + \hat{H}_{\rm ph} + \hat{H}_{\text{ex-ph}}, \tag{1}$$

where $\hat{H}_{\rm ex}$ is the Hamiltonian of excitons in graphene in the presence of the gap, $\hat{H}_{\rm ph}$ is the Hamiltonian of the microcavity photons, and $\hat{H}_{\text{ex-ph}}$ is the Hamiltonian for the exciton-photon interaction.

The Hamiltonian of 2D excitons in the graphene in the presence of a gap is given by

$$\hat{H}_{\rm ex} = \hat{H}^{(0)}_{\rm ex} + \hat{H}_{\text{ex-ex}}, \tag{2}$$

where $\hat{H}^{(0)}_{\rm ex}$ is the Hamiltonian of noninteracting 2D excitons in gapped graphene and $\hat{H}_{\text{ex-ex}}$ is the Hamiltonian of the exciton-exciton interaction.

The Hamiltonian of noninteracting excitons in gapped graphene $\hat{H}^{(0)}_{\rm ex}$ is given by

$$\hat{H}^{(0)}_{\rm ex} = \sum_{\mathbf{P}} \epsilon_{\rm ex}(P)\hat{b}^{\dagger}_{\mathbf{P}}\hat{b}_{\mathbf{P}}, \tag{3}$$

where $\hat{b}^{\dagger}_{\mathbf{P}}$ and $\hat{b}_{\mathbf{P}}$ are the excitonic creation and annihilation operators obeying Bose commutation relations and $\epsilon_{\rm ex}(P)$ is the energy dispersion of a single exciton in a graphene layer.

The Hamiltonian of the exciton-exciton interaction $\hat{H}_{\text{ex-ex}}$ in graphene in the presence of a gap is given by

$$\hat{H}_{\text{ex-ex}} = \frac{1}{2A}\sum_{\mathbf{P},\mathbf{P}',\mathbf{q}} U_{\mathbf{q}}\hat{b}^{\dagger}_{\mathbf{P}+\mathbf{q}}\hat{b}^{\dagger}_{\mathbf{P}'-\mathbf{q}}\hat{b}_{\mathbf{P}}\hat{b}_{\mathbf{P}'}, \tag{4}$$

where A is the macroscopic quantization area and $U_{\mathbf{q}}$ is the Fourier transform of the exciton-exciton pair repulsion potential.

The Hamiltonian of photons in a semiconductor microcavity is given by[24]

$$\hat{H}_{\rm ph} = \sum_{\mathbf{P}} \epsilon_{\rm ph}(P)\hat{a}^{\dagger}_{\mathbf{P}}\hat{a}_{\mathbf{P}}, \tag{5}$$

where $\hat{a}^{\dagger}_{\mathbf{P}}$ and $\hat{a}_{\mathbf{P}}$ are photonic creation and annihilation Bose operators, and $\epsilon_{\rm ph}(P)$ is the cavity photon energy dispersion.

Following Ref. 25 the Hamiltonian of the harmonic exciton-photon coupling can be written as

$$\hat{H}_{\text{ex-ph}} = \hbar\Omega_R \sum_{\mathbf{P}} \hat{a}^{\dagger}_{\mathbf{P}}\hat{b}_{\mathbf{P}} + \text{H.c.}, \tag{6}$$

where the exciton-photon coupling energy is represented by the Rabi splitting $\hbar\Omega_R$.

Let us present the detailed consideration and analysis of each term in Eq. (1): first, the excitonc Hamiltonian $\hat{H}_{\rm ex}$ that describes the formation of excitons in gapped graphene; second, the Hamiltonian $\hat{H}_{\rm ph}$ that describes the microcavity photons; and last, the Hamiltonian $\hat{H}_{\text{ex-ph}}$responsible for the exciton-photon coupling within the microcavity.

III. EXCITONIC HAMILTONIAN

In this section we present the excitonic Hamiltonian $\hat{H}_{\rm ex}$ that consists from two terms: the Hamiltonian that describes the formation of the gas of noninteracting excitons in gapped graphene and the Hamiltonian responsible for the exciton-exciton interaction that we assume is strong enough to be neglected.

A. An exciton in a graphene layer in the presence of the gap

The Hamiltonian of 2D excitons in gapped graphene is given by Eq. (2). As the first step let us analyze the Hamiltonian of noninteracting excitons $\hat{H}^{(0)}_{\rm ex}$. As follows from Eq. (3), this Hamiltonian is determined by the energy-momentum dispersion of noninteracting excitons $\epsilon_{\rm ex}(P)$. Therefore, we need to find out the energy-momentum dispersion $\epsilon_{\rm ex}(P)$ of the electron and hole that are bound in a gapped graphene layer via an electromagnetic attraction by solving a two-body problem.

We consider an electron and a hole located in a single graphene sheet, assume that they form an exciton, and introduce the gap parameter δ. The gap parameter δ is the consequence of adatoms on the graphene sheets (e.g, by hydrogen, oxygen or other noncarbon atoms[8]) which create a one-particle potential.

We use the coordinate vectors of the electron and the hole $\mathbf{r}_1$ and $\mathbf{r}_2$, respectively. Each honeycomb lattice is characterized by the coordinates $(\mathbf{r}_j,1)$ on sublattice A and $(\mathbf{r}_j,2)$ on sublattice B. Then wave function, describing two particles in the same graphene sheet, reads $\Psi(\mathbf{r}_1,s_1;\mathbf{r}_2,s_2)$. This wave function can also be understood as a four-component spinor, where the spinor components refer to the four possible values of the sublattice indices s_1,s_2:

$$\Psi(\mathbf{r}_1,s_1;\mathbf{r}_2,s_2) = \begin{pmatrix} \phi_{aa}(\mathbf{r}_1,\mathbf{r}_2) \\ \phi_{ab}(\mathbf{r}_1,\mathbf{r}_2) \\ \phi_{ba}(\mathbf{r}_1,\mathbf{r}_2) \\ \phi_{bb}(\mathbf{r}_1,\mathbf{r}_2) \end{pmatrix}. \tag{7}$$

The Hamiltonian that describes the interacting electron and hole with a broken sublattice symmetry can be written as

$$\mathcal{H} = \begin{pmatrix} V(r) & d_2 & d_1 & 0 \\ d_2^\dagger & -2\delta + V(r) & 0 & d_1 \\ d_1^\dagger & 0 & 2\delta + V(r) & d_2 \\ 0 & d_1^\dagger & d_2^\dagger & V(r) \end{pmatrix}, \quad (8)$$

where $V(r)$ is the electron-hole electromagnetic interaction that depends on $r = |\mathbf{r}_1 - \mathbf{r}_2|$. In Eq. (8), $d_j = \hbar v_F(-i\partial_{x_j} - \partial_{y_j})$, $d_j^\dagger = \hbar v_F(-i\partial_{x_j} + \partial_{y_j})$, where $\partial_{x_j} = \partial/\partial x_j$, $\partial_{y_j} = \partial/\partial y_j$, $j = 1,2$, x and y are components of the vectors $\mathbf{r}_1$ and $\mathbf{r}_2$, and $v_F = \sqrt{3}at/(2\hbar)$ is the Fermi velocity of electrons in graphene, where $a = 2.46$ Å is a lattice constant and the value of the overlap integral between the nearest carbon atoms is $t \approx 2.71$ eV.[26] In Eq. (8) we take into account the renormalization of the electron-hole distance in the electron-hole Coulomb attraction due to the non-locality of electron and hole wave function, assuming the following model for the electron-hole attraction: $V(r) = -e^2/[4\pi\varepsilon_0\varepsilon(r^2 + r_0^2)^{1/2}]$, where $\varepsilon_0 = 8.85 \times 10^{-12}$ C^2/(Nm^2), e is the electron charge, $\varepsilon = 2.5$ is the dielectric constant of graphene, and r_0 is the renormalization parameter which will be estimated below. It should be mentioned that the main contribution to the polariton mass is the cavity photon mass rather than exciton mass, and, therefore, we use our model to estimate the exciton mass roughly by the order of magnitude. Assuming $r \ll r_0$, we expand $V(r)$ in a Taylor series as $V(r) = -V_0 + \gamma r^2$, where $V_0 = e^2/(4\pi\varepsilon\varepsilon_0 r_0)$ and $\gamma = e^2/(8\pi\varepsilon_0\varepsilon r_0^3)$.

Now we have to solve the eigenvalue problem for the Hamiltonian (8) $\mathcal{H}\Psi = \epsilon\Psi$ and find the energy of the exciton ϵ. The eigenfunction depends on the coordinates of both particles, namely $(\mathbf{r}_1,\mathbf{r}_2)$. To separate the relative motion of the electron and hole we use the following ansatz for the wave function:

$$\Psi_j(\mathbf{R},\mathbf{r}) = \mathrm{e}^{i\mathbf{P}\cdot\mathbf{R}/\hbar}\ \psi_j(\mathbf{r}), \quad (9)$$

where $\mathbf{P}$ is momentum, and following Ref. 21 for a generalized center-of-mass coordinate $\mathbf{R}$ and relative coordinate $\mathbf{r}$ we have

$$\mathbf{R} = \alpha\mathbf{r}_1 + \beta\mathbf{r}_2, \quad \mathbf{r} = \mathbf{r}_1 - \mathbf{r}_2 \quad (10)$$

with the parameters

$$\alpha = \frac{\epsilon - 2\delta}{2\epsilon}, \quad \beta = \frac{\epsilon + 2\delta}{2\epsilon} \quad (11)$$

that have been found from the condition of separation of the relative motion of the electron-hole pair and the motion of the center of mass. The procedure given in Ref. 21 can be applied to the eigenvalue problem $(\mathcal{H} + V_0)\Psi = (\epsilon + V_0)\Psi$ when we assume that both relative and center-of-mass kinetic energies, as well as the harmonic term in the potential energy $V(r) + V_0 = \gamma r^2$, are small in comparison to the gap energy 2δ. Starting from the wave function (9) and using the same procedure that we developed in Ref. 21, we obtain for the spinor component ϕ_{aa} the equation

$$\left(\frac{(v_F P)^2}{2\epsilon} + \gamma r^2 - \frac{2\epsilon(\hbar v_F)^2\nabla_{\mathbf{r}}^2}{(\epsilon^2 - 4\delta^2)}\right)\phi_{aa} = (\epsilon + V_0)\,\phi_{aa}. \quad (12)$$

The last equation can be rewritten in more convenient form,

$$\left(-\mathcal{F}\nabla_r^2 + \gamma r^2\right)\phi_{aa} = \mathcal{F}_0\phi_{aa}, \quad (13)$$

where $\mathcal{F}$ is given by

$$\mathcal{F} = \frac{2(\epsilon + V_0)(\hbar v_F)^2}{(\epsilon + V_0)^2 - 4\delta^2} \quad (14)$$

and $\mathcal{F}_0$ is given by

$$\mathcal{F}_0 = \epsilon + V_0 - \frac{(v_F P)^2}{2(\epsilon + V_0)}. \quad (15)$$

Equation (13) describes a two-dimensional isotropic harmonic oscillator, whose solutions are given by the condition

$$\frac{\mathcal{F}_0}{\mathcal{F}} = 2N\sqrt{\frac{\gamma}{\mathcal{F}}}, \quad (16)$$

with $N = 2n_1 + n_2 + 1$ and quantum numbers $n_1 = 0,1,2,3,\ldots$ and $n_2 = 0, \pm 1, \pm 2, \pm 3, \ldots, \pm n_1$. Below we will focus subsequently on the analysis of the ground state of the exciton corresponding to $N = 1$. At $N = 1$ from Eq. (16), by keeping the second-order terms with respect to P, we obtain

$$\epsilon'^4 - [4\delta^2 + (v_F P)^2]\epsilon'^2 - 8C\epsilon' + 4\delta^2(v_F P)^2 = 0, \quad (17)$$

where $\epsilon' = \epsilon + V_0$ and $C = \gamma(\hbar v_F)^2$.

Assuming $C \ll \epsilon(\epsilon^2 - 4\delta^2)$, we solve Eq. (17) for ϵ, then expand ϵ up to the second order in P (i.e. for $v_F P \ll \delta$) and the first order in C and obtain for the electron-hole dispersion

$$\epsilon(P) = 2\delta + \epsilon_{\mathrm{ex}}(P), \quad (18)$$

where the exciton dispersion presented in Eq. (3) is given by

$$\epsilon_{\mathrm{ex}}(P) = -V_0 + \frac{C}{\delta^2} + \frac{P^2}{2\mathcal{M}}. \quad (19)$$

In Eq. (19) $\mathcal{M}$ is the effective exciton mass given by

$$\mathcal{M} = \frac{2\delta^4}{Cv_F^2}. \quad (20)$$

The exciton effective mass $\mathcal{M}$ increases when the gap parameter δ increases. Note that, if $N > 1$, at small momenta P the exciton energy spectrum at the same quantum number N increases with the increase of the gap δ. However, the exciton energy spectrum at the same gap energy δ decreases with the increase of the quantum number N.

The exciton radius can be obtained from the wave function of the 2D harmonic oscillator and reads $\rho = 2^{-1/2}[\mathcal{F}(\epsilon)/\gamma]^{1/4}$. In the dilute system when the majority of particles are in a condensate, we substitute ϵ at zero momentum: $\epsilon(P = 0)$.

The electron-hole recombination produces a photon with energy $E_{\mathrm{ph}} = \hbar\omega$ equal, by energy conservation, to the exciton excitation energy $2\delta + \epsilon_{\mathrm{ex}}(0)$. Then the renormalization parameter r_0 can be found from the condition $\hbar\omega = 2\delta + \epsilon_{\mathrm{ex}}(0)$, where $\epsilon_{\mathrm{ex}}(P)$ is given by Eq. (19). This condition leads to the following equation for r_0:

$$2\delta^2(2\delta - \hbar\omega)r_0^3 - 2D\delta^2 r_0^2 + D(\hbar v_F)^2 = 0, \quad (21)$$

where $D = e^2/(4\pi\varepsilon_0\varepsilon)$. For dipolar excitons in GaAs/AlGaAs coupled quantum wells, the energy of the recombination peak is $\hbar\omega = 1.61$ eV.[27] We expect similar photon energies in graphene; its exact value depends on the graphene dielectric environment and substrate properties though.

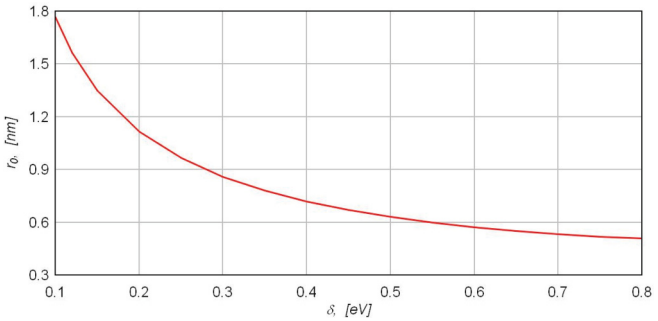

FIG. 1. (Color online) The dependence of the parameter r_0 on the gap energy δ.

The parameter r_0 is obtained as a result of a numerical solution of Eq. (21) for each value of the gap energy. The results of calculations are presented in Fig. 1. According to Fig. 1, the parameter r_0 decreases when the gap energy δ increases.

B. Exciton-exciton interaction

Here we analyze the Hamiltonian (4) of the exciton-exciton interaction $H_{\text{ex-ex}}$ in graphene in the presence of the gap, which contributes to the exciton Hamiltonian $\hat{H}_{\text{ex}}$ given by Eq. (2). As discussed in Refs. 28 and 29 for a dilute exciton gas, the excitons can be treated as bosons with a repulsive contact interaction. For small wave vectors $q \ll \rho^{-1}$, the value of $U_{\mathbf{q}}$ which is related to exciton-exciton repulsion can be approximated as

$$U_{\mathbf{q}} \simeq U = \frac{3e^2\rho}{2\pi\varepsilon_0\varepsilon}. \tag{22}$$

This approximation for the exciton-exciton repulsion is applicable because resonantly excited excitons have very small wave vectors.[25] Another reason for the validity of this approximation is that the exciton gas is assumed to be very dilute and the average distance between excitons $r_s \gg \rho$, which implies the characteristic wave number $q \sim r_s^{-1} \ll \rho^{-1}$. A much smaller contribution to the exciton-exciton interaction is also given by band-filling saturation effects,[30] which are neglected here. To demonstrate the dependence of U on the gap energy, we calculate U for each value of ρ that is by itself the function of the parameter r_0 obtained from Eq. (21). The result of the numerical calculations presented in Fig. 2 shows that U decreases when the gap energy δ increases.

IV. MICROCAVITY PHOTONS

The Hamiltonian of photons in a semiconductor microcavity is determined by the cavity photon energy dispersion $\epsilon_{\text{ph}}(P)$. According to Ref. 24 this dispersion is defined as $\epsilon_{\text{ph}}(P) = (c/\sqrt{\varepsilon_{\text{cav}}})\sqrt{P^2 + \hbar^2\pi^2 L_c^{-2}}$, where ε_{cav} is the dielectric constant of the cavity, c is the speed of light in vacuum, and L_c is the length of the microcavity.

Embedding graphene in an optical microcavity can lead to the formation of polaritons when the excitons couple to the cavity photons. In such cases the microcavity consists of two mirrors parallel to each other and a graphene sheet placed in between. Then the photons are confined in the direction

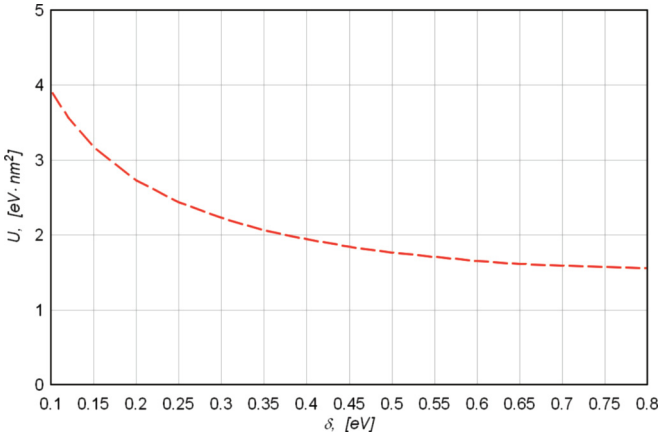

FIG. 2. (Color online) The dependence of U on the gap energy δ.

perpendicular to the mirrors, but move freely in the two directions parallel to the mirrors. The length of the microcavity is chosen as

$$L_c = \frac{\hbar\pi c}{(2\delta - V_0 + C/\delta^2)\sqrt{\varepsilon_{\text{cav}}}} \tag{23}$$

with the resonance condition that the photonic and excitonic branches are equal at $P = 0$, i.e., for $\epsilon(0) = \epsilon_{\text{ph}}(0)$. This resonance condition can be achieved either by controlling the gap energy δ or by choosing the appropriate length L_c of the microcavity.

V. EXCITON-PHOTON INTERACTION

The Hamiltonian of the harmonic exciton-photon coupling, Eq. (6), contributes to the total Hamiltonian (1) of the system. In this Hamiltonian the exciton-photon coupling energy is represented by the Rabi splitting $\hbar\Omega_R$. Neglecting anharmonic terms for the exciton-photon coupling, the Rabi splitting $\hbar\Omega_R$ can be estimated quasiclassically as

$$|\hbar\Omega_R| = |\langle f|\hat{H}_{\text{int}}|i\rangle|, \tag{24}$$

where $\hat{H}_{\text{int}}$ is the Hamiltonian of the electron-photon interaction. The initial state $|i\rangle$ corresponds to the valence band filled by electrons and the empty conduction band, while the final state $|f\rangle$ corresponds to one hole in the valence band and one electron in the conduction band. In Eq. (24) the initial $|i\rangle$ and final $|f\rangle$ electron states are defined as

$$|i\rangle = \prod_{\mathbf{q}} \hat{c}_{\mathbf{q}}^{(v)\dagger}|0\rangle_v|0\rangle_c, \quad |f\rangle = \hat{b}_{\mathbf{q}}^{\dagger}|i\rangle. \tag{25}$$

In Eq. (25), $\hat{c}_{\mathbf{q}}^{(v)\dagger}$ is the Fermi creation operator of the electron in the valence band with the wave vector $\mathbf{q}$, $|0\rangle_c$ denotes the wave function of the vacuum in the conduction band, $\prod_{\mathbf{q}} \hat{c}_{\mathbf{q}}^{(v)\dagger}|0\rangle_v$ corresponds to the completely filled valence band, and $\hat{b}_{\mathbf{q}}^{\dagger}$ is the exciton creation operator with the electron in the conduction band c and the hole in the valence band v. Following Ref. 31, $\hat{b}_{\mathbf{q}}$ and $\hat{b}_{\mathbf{q}}^{\dagger}$ for this case are defined as

$$\hat{b}_{\mathbf{q}} = \sum_{\mathbf{q}'} \hat{c}_{\mathbf{q}-\mathbf{q}'}^{(v)\dagger}\hat{c}_{\mathbf{q}'}^{(c)}, \quad \hat{b}_{\mathbf{q}}^{\dagger} = \sum_{\mathbf{q}'} \hat{c}_{\mathbf{q}'}^{(c)\dagger}\hat{c}_{\mathbf{q}-\mathbf{q}'}^{(v)}. \tag{26}$$

where $\hat{c}_{\mathbf{q}}^{(c)\dagger}$ and $\hat{c}_{\mathbf{q}}^{c}$ are the Fermi creation and annihilation operators of the electron in the conduction band with the the wave vector $\mathbf{q}$. The eigenfunctions and eigenenergies of an electron in graphene in the presence of a gap are given in Appendix A. For graphene the electron-photon interaction Hamiltonian is determined as

$$\hat{H}_{\text{int}} = -v_F e\boldsymbol{\sigma}\cdot\mathbf{A}_{ph0} = \frac{v_F e}{i\omega}\boldsymbol{\sigma}\cdot\mathbf{E}_{ph0}, \tag{27}$$

where $\boldsymbol{\sigma} = (\sigma_x,\sigma_y)$ are Pauli matrices, $\mathbf{A}_{ph0}$ is the electromagnetic vector potential of a single cavity photon, and $E_{ph0} = [\hbar\omega/(2\varepsilon_0\varepsilon_{\text{cav}}W)]^{1/2}$ is the magnitude of electric field corresponding to a single cavity photon with frequency ω within the microcavity volume W.

Substituting Eqs. (26), (A3), and (A4) into (25) and using the electron-photon interaction $\hat{H}_{\text{int}}$ (27), we finally obtain from Eq. (24)

$$|\hbar\Omega_R| = \left|\frac{ev_F}{i\omega}\int dx\int dy\left[\psi^*_{c,E_c}(x,y)\boldsymbol{\sigma}\cdot\mathbf{E}_{ph0}\psi_{v,E_v}(x,y)\right]\right| = \left|\frac{ev_F}{2i\omega}\sqrt{\frac{\delta^2-E^2}{E^2}}\left[E_{ph0x}\left(\frac{\hbar v_F(q_x+iq_y)}{\delta-E}+\frac{\hbar v_F(q_x-iq_y)}{\delta+E}\right)\right.\right.$$
$$\left.\left.+\,iE_{ph0y}\left(\frac{-\hbar v_F(q_x+iq_y)}{\delta-E}+\frac{\hbar v_F(q_x-iq_y)}{\delta+E}\right)\right]\right|. \tag{28}$$

After simplification of Eq. (28) we obtain

$$|\hbar\Omega_R| = \frac{e\hbar v_F^2}{\omega E\sqrt{\delta^2-E^2}}\sqrt{(q_xE_{ph0x}+q_yE_{ph0y})^2\delta^2+(q_yE_{ph0x}-q_xE_{ph0y})^2E^2}. \tag{29}$$

Assuming for simplicity an electric field corresponding to a single cavity photon mode is directed along the x axis, we obtain

$$|\hbar\Omega_R| = \frac{ev_F}{\sqrt{\delta^2+\hbar^2v_F^2q^2}}\sqrt{\frac{\hbar}{2W\varepsilon_0\varepsilon_{\text{cav}}\omega}}\frac{\sqrt{q_x^2\delta^2+q_y^2E^2}}{|q|}. \tag{30}$$

In the limit $q\to 0$, when $\omega = 2\delta/\hbar$, we obtain from Eq. (30)

$$|\hbar\Omega_R| = \hbar v_F e\sqrt{\frac{1}{2W\varepsilon_0\varepsilon_{\text{cav}}\delta}}, \tag{31}$$

where $W = L_cS$ is the volume of a system with the area S. When L_c is obtained from the condition of the resonance of the exciton, and the corresponding photon mode is presented by Eq. (23), we obtain for the Rabi splitting

$$|\hbar\Omega_R| = \hbar v_F e\sqrt{\frac{2-V_0\delta^{-1}+C\delta^{-3}}{2\pi\varepsilon_0\hbar c\sqrt{\varepsilon_{\text{cav}}}S}}. \tag{32}$$

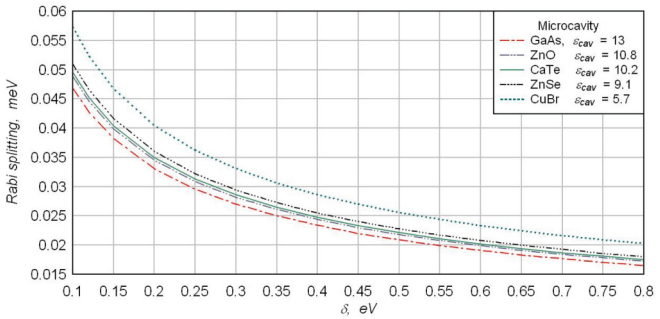

FIG. 3. (Color online) The dependence of the Rabi splitting $|\hbar\Omega_R|$ on the gap energy δ for microcavities with the different dielectric constants ε_{cav}.

According to Eq. (32), Rabi splitting depends on the gap energy δ, the area of the microcavity S, and the dielectric constant of the microcavity ε_{cav}. The microcavity can be formed in different types of semiconductors. By using a different semiconductor for the Bragg mirrors used to confine the photon in the microcavity, there are possibilities to further increase the Rabi splitting. In our calculations we considered the microcavities that were fabricated for the experimental studies of microcavity polaritons.[32–42] The results of the calculations of the dependence of Rabi splitting on the gap energy δ for the microcavities with different dielectric constants are presented in Fig. 3. In the calculations according to the experiment presented in Ref. 43 we used the value $S = 10\,\mu\text{m}^2$ for the area of the microcavity. The analysis of the results in Fig. 3 shows that Rabi splitting decreases when the gap energy δ increases, while for the same gap energy the larger value of the microcavity dielectric constant there corresponds to a smaller value of the Rabi splitting. Therefore, we can conclude that a proper choice of the semiconductor materials for Bragg mirrors for the fabrication of the microcavity is very important, and allows achieving a larger value for the Rabi splitting for the same gap energy.

VI. SUPERFLUIDITY OF MICROCAVITY POLARITONS

We can diagonalize the linear part of the total Hamiltonian $\hat{H}_{\text{tot}}$ [without the second term on the right-hand side of Eq. (2)] by applying the unitary transformations,[25] and as the result obtain (see Appendix B)

$$\hat{H}_0 = \sum_{\mathbf{P}} E_{LP}(P)\hat{l}_{\mathbf{P}}^{\dagger}\hat{l}_{\mathbf{P}} + \sum_{\mathbf{P}} E_{UP}(P)\hat{u}_{\mathbf{P}}^{\dagger}\hat{u}_{\mathbf{P}}, \tag{33}$$

where $\hat{l}_{\mathbf{P}}^{\dagger}$, $\hat{l}_{\mathbf{P}}$ and $\hat{u}_{\mathbf{P}}^{\dagger}$, $\hat{u}_{\mathbf{P}}$ are the Bose creation and annihilation operators for the lower and upper polaritons, respectively. The corresponding energy spectra $E_{LP}(P)$ and $E_{UP}(P)$ of the lower and upper polaritons are given by Eq. (B3).

The substitution of the polaritonic representation of the excitonic and photonic operators (B1) into the total Hamiltonian (1), gives the Hamiltonian of the lower polaritons:[25]

$$\hat{H}_{\rm tot} = \sum_{\mathbf{P}} E_{LP}(P)\hat{l}^{\dagger}_{\mathbf{P}}\hat{l}_{\mathbf{P}} + \frac{1}{2A}\sum_{\mathbf{P},\mathbf{P}',\mathbf{q}} \tilde{W}_{\mathbf{P},\mathbf{P}',\mathbf{q}}\hat{l}^{\dagger}_{\mathbf{P}+\mathbf{q}}\hat{l}^{\dagger}_{\mathbf{P}'-\mathbf{q}}\hat{l}_{\mathbf{P}}\hat{l}_{\mathbf{P}'}, \tag{34}$$

where the effective polariton-polariton interaction $\tilde{W}$ is given by

$$\tilde{W}_{\mathbf{P},\mathbf{P}',\mathbf{q}} = U X_{\mathbf{P}+\mathbf{q}} X_{\mathbf{P}'} X_{\mathbf{P}'-\mathbf{q}} X_{\mathbf{P}}, \tag{35}$$

with $U = 3e^2\rho/(2\pi\varepsilon_0\varepsilon)$ defined in Sec. III B.

At small momenta $\alpha \equiv 1/2[\mathcal{M}^{-1} + (c/\sqrt{\varepsilon_{\rm cav}})L_c/\hbar\pi]P^2/|\hbar\Omega_R| \ll 1$, the single-particle lower polariton spectrum obtained from Eq. (B3), in linear order with respect to the small parameter α, is

$$E_{LP}(P) \approx \frac{c}{\sqrt{\varepsilon_{\rm cav}}}\hbar\pi L_c^{-1} - |\hbar\Omega_R| + \frac{P^2}{2M_p}, \tag{36}$$

where M_p is the effective mass of polariton given by

$$M_p = 2\left(\mathcal{M}^{-1} + \frac{cL_c}{\sqrt{\varepsilon_{\rm cav}}\hbar\pi}\right)^{-1}. \tag{37}$$

If we take into account only the lower polaritons corresponding to the lower energy at $P = 0$ and measure energy relative to the lower polariton energy $(c/\sqrt{\varepsilon_{\rm cav}})\hbar\pi L_c^{-1} - |\hbar\Omega_R|$ the resulting effective Hamiltonian for polaritons has the form

$$\hat{H}_{\rm eff} = \sum_{\mathbf{P}} \frac{P^2}{2M_p}\hat{l}^{\dagger}_{\mathbf{P}}\hat{l}_{\mathbf{P}} + \frac{U^{(0)}_{\rm eff}}{2A}\sum_{\mathbf{P},\mathbf{P}',\mathbf{q}} \hat{l}^{\dagger}_{\mathbf{P}+\mathbf{q}}\hat{l}^{\dagger}_{\mathbf{P}'-\mathbf{q}}\hat{l}_{\mathbf{P}}\hat{l}_{\mathbf{P}'}, \tag{38}$$

where $U^{(0)}_{\rm eff} = \frac{1}{4}U = 3e^2\rho/(8\pi\varepsilon_0\varepsilon)$, since at small momenta $|X_P|^2 \approx |C_P|^2 \approx 1/2$.

In the dilute limit ($n\rho^2 \ll 1$, where n is the 2D polariton density), at zero temperature Bose-Einstein condensation of polaritons appears in the system, since the Hamiltonian of microcavity polaritons (38) corresponds to the weakly interacting Bose gas. The Bogoliubov approximation for the dilute weakly interacting Bose gas of polaritons results in the sound spectrum of collective excitations at low momenta:[44,45] $\varepsilon(P) = c_S P$ with the sound velocity $c_S = (U^{(0)}_{\rm eff}n/M_p)^{1/2} = (3e^2\rho n/(8\pi\varepsilon_0\varepsilon M_p))^{1/2}$.

The dilute polaritons constructed by excitons in gapped graphene embedded in the optical microcavity and microcavity photons form a 2D weakly interacting gas of bosons with pair short-range repulsion. So the superfluid-normal phase transition in this system is the Kosterlitz-Thouless transition,[46] and the temperature of this transition T_c in a two-dimensional microcavity polariton system is determined by the equation

$$T_c = \frac{\pi\hbar^2 n_s(T_c)}{2k_B M_p}, \tag{39}$$

where $n_s(T)$ is the superfluid density of the polariton system in a microcavity as a function of temperature T, and k_B is Boltzmann constant. We obtain the superfluid density as $n_s = n - n_n$ by determining the density of the normal component n_n when we follow the procedure[44] as a linear response of the total momentum with respect to the external velocity:

$$n_s = n - \frac{3\zeta(3)}{2\pi\hbar^2}\frac{sk_B^3T^3}{c_S^4 M_p}, \tag{40}$$

where $s = 4$ is the spin degeneracy factor.

Substituting Eq. (40) for the density n_s of the superfluid component into Eq. (39), we obtain an equation for the Kosterlitz-Thouless transition temperature T_c. The solution of this equation is

$$T_c = \left[\left(1 + \sqrt{\frac{32}{27}\left(\frac{M_p k_B T_c^0}{\pi\hbar^2 n}\right)^3 + 1}\right)^{1/3} - \left(\sqrt{\frac{32}{27}\left(\frac{M_p k_B T_c^0}{\pi\hbar^2 n}\right)^3 + 1} - 1\right)^{1/3}\right]\frac{T_c^0}{2^{1/3}}, \tag{41}$$

where T_c^0 is the temperature at which the superfluid density vanishes in the mean-field approximation [i.e., $n_s(T_c^0) = 0$],

$$T_c^0 = \frac{1}{k_B}\left(\frac{\pi\hbar^2 n c_s^4 M_p}{6s\zeta(3)}\right)^{1/3}. \tag{42}$$

The analysis of Eq. (41) shows that the Kosterlitz-Thouless transition temperature T_c depends on the polariton density, the gap energy, as well as on the properties of the microcavity. Figures 4 and 5 represent the results of the calculations for the Kosterlitz-Thouless transition temperature T_c as a function of the gap energy δ at the different fixed polariton densities n.

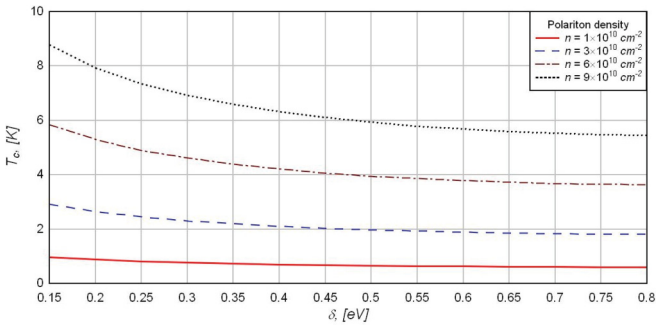

FIG. 4. (Color online) The dependence of the Kosterlitz-Thouless transition temperature T_c on the gap energy δ for the different polariton densities for a GaAs microcavity.

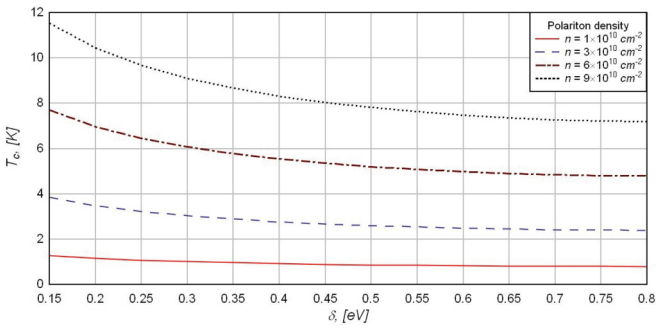

FIG. 5. (Color online) The dependence of the Kosterlitz-Thouless transition temperature T_c on the gap energy δ for the different polariton densities for a CuBr microcavity.

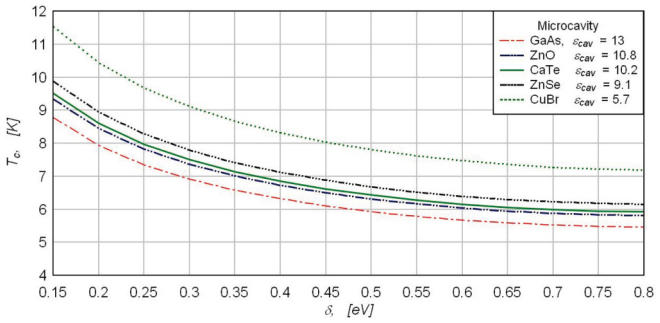

FIG. 6. (Color online) The dependence of the Kosterlitz-Thouless transition temperature T_c on the gap energy δ for microcavities with the different dielectric constants $\varepsilon_{\rm cav}$.

We consider the graphene layer that is embedded in the GaAs and CuBr microcavities with the dielectric constants $\varepsilon_{\rm cav} = 13$ and $\varepsilon_{\rm cav} = 5.7$, respectively. According to Figs. 4 and 5, at the same polariton density n, T_c decreases when δ increases, and at the same gap energy δ the transition temperature T_c increases when the polariton density n increases. A proper choice of the semiconductor materials for fabrication of the microcavities is important to achieve a high Kosterlitz-Thouless transition temperature. We consider the graphene layer embedded in the different microcavities and calculate the Kosterlitz-Thouless transition temperature T_c as a function of the gap energy using different dielectric constants $\varepsilon_{\rm cav}$ for microcavities that were fabricated for the observation of polaritons experimentally.[32–42] The results of calculations for the polariton density $n = 9 \times 10^{10}$ cm^{-2} presented in Fig. 6 show that the Kosterlitz-Thouless transition temperature T_c is higher for the microcavity fabricated with the material that has smaller dielectric constant.

VII. DISCUSSION

According to Eq. (37), the effective polariton mass M_p is mostly determined by the size of the microcavity, which depends on the gap energy δ according to Eq. (23) when the exciton and microcavity photon branches of the spectrum are in resonance at zero momentum. The gap dependence of the sound velocity is caused by the gap dependence of the exciton-exciton interaction described in Sec. III B. According to Figs. 4–6 we conclude that Kosterlitz-Thouless temperature T_c and, therefore, according to Eq. (39) superfluid density n_s, are decreasing functions of the gap energy δ in graphene and increasing functions of the polariton density n, while the Kosterlitz-Thouless transition temperature is higher for the microcavity fabricated with the material that has smaller dielectric constant.

The superfluidity and BEC of polaritons formed by quantum-well excitons and microcavity photons have been discussed widely. The comparison shows that the advantage of observing the superfluidity and BEC of polaritons formed by the gapped graphene excitons and microcavity photons is related to the fact that in this system the superfluidity and BEC of polaritons can be controlled by the gap.

In conclusion, we propose the superfluidity of 2D exciton polaritons formed by gapped graphene excitons and microcavity photons, when the gapped graphene layer is embedded in an optical microcavity. We conclude that the Rabi splitting decreases when gap energy δ increases, while for the same gap energy the larger value of the dielectric constant of the microcavity gives a smaller value for the Rabi splitting. We show that the Kosterlitz-Thouless temperature and the superfluid density increases with the rise of the polariton density and decreases with the rise of the gap energy due to δ dependence of the sound velocity of collective excitations, while T_c is higher for the microcavity fabricated with the material that has smaller dielectric constant $\varepsilon_{\rm cav}$. Thus, the Kosterlitz-Thouless temperature and the superfluid density could be controlled by n, δ, and $\varepsilon_{\rm cav}$.

ACKNOWLEDGMENTS

The authors acknowledge support from the Center for Theoretical Physics of the New York City College of Technology, CUNY, and from the Deutsche Forschungsgemeinschaft through Grant No. ZI 305/5-1. The authors thank the referee for valuable recommendations.

APPENDIX A:THE EIGENFUNCTIONS AND EIGENENERGIES OF AN ELECTRON IN GRAPHENE IN THE PRESENCE OF A GAP

We consider two fermions and ignore their interaction [i.e., $V(r) = 0$]. The electrons in the conduction band, described by the spinor wave function $\psi_{cE}(x,y)$, and the holes in the valence band, described by the spinor wave function $\psi_{vE'}(x,y)$, are solutions of the eigenvalue equations

$$H_{-\delta}\psi_{cE} = E\psi_{cE}, \quad H_{\delta}\psi_{vE'} = -E'\psi_{vE'} \tag{A1}$$

of the Dirac-Weyl Hamiltonian

$$H_{\delta} = \begin{pmatrix} \delta & \hbar v_F(\partial_x - i\partial_y) \\ \hbar v_F(\partial_x + i\partial_y) & -\delta \end{pmatrix}. \tag{A2}$$

In the presence of a gap 2δ, these solutions are

$$\psi_{cE}(x,y) = \sqrt{\frac{\delta - E}{2E}}\frac{\exp[i(q_x x + q_y y])}{\sqrt{L_x L_y}}\begin{pmatrix} \frac{\hbar v_F(q_x - iq_y)}{\delta - E} \\ 1 \end{pmatrix}, \tag{A3}$$

$$\psi_{vE}(x,y) = \sqrt{\frac{\delta + E}{2E}}\frac{\exp[i(q_x x + q_y y)]}{\sqrt{L_x L_y}}\begin{pmatrix} \frac{\hbar v_F(q_x - iq_y)}{\delta + E} \\ 1 \end{pmatrix}, \tag{A4}$$

where $E = \sqrt{\delta^2 + \hbar^2 v_F^2 q^2}$ is the energy of the electron or the hole, and L_x and L_y are the 2D microcavity dimensions. This allows us to construct the four components of the spinor in Eq. (7) from the solutions of Eq. (A1) as

$$\phi_{jk}(\mathbf{r}_1,\mathbf{r}_2) = \psi_{cE,j}(\mathbf{r}_1)\psi_{vE',k}(\mathbf{r}_2) \quad (j = a,b; k = a,b), \tag{A5}$$

which solves the eigenvalue equation for two noninteracting particles with the Hamiltonian $\mathcal{H}$ in Eq. (8) when $V(r) = 0$: $\mathcal{H}_0\Psi = (E - E')\Psi$, where $\mathcal{H}_0$ is the Hamiltonian of two noninteracting particles.

APPENDIX B: THE REPRESENTATION OF POLARITON OPERATORS FOR THE HAMILTONIAN OF THE EXCITON-PHOTON SYSTEM IN A MICROCAVITY

We express the exciton and microcavity photon operators in terms of polariton operators. The exciton and photon operators are defined as[25]

$$\hat{b}_{\mathbf{P}} = X_P \hat{l}_{\mathbf{P}} - C_P \hat{u}_{\mathbf{P}}, \quad \hat{a}_{\mathbf{P}} = C_P \hat{l}_{\mathbf{P}} + X_P \hat{u}_{\mathbf{P}}, \tag{B1}$$

where $\hat{l}_{\mathbf{P}}$ and $\hat{u}_{\mathbf{P}}$ are lower and upper polariton Bose operators, respectively, X_P and C_P are

$$X_P = \left[1 + \left(\frac{\hbar\Omega_R}{E_{LP}(P) - \epsilon_{\mathrm{ph}}(P)}\right)\right]^{-1/2}, \quad C_P = -\left[1 + \left(\frac{E_{LP}(P) - \epsilon_{\mathrm{ph}}(P)}{\hbar\Omega_R}\right)\right]^{-1/2}, \tag{B2}$$

and the energy dispersion of the lower and upper polaritons are

$$E_{LP/UP}(P) = \frac{\epsilon_{\mathrm{ph}}(P) + \epsilon_{\mathrm{ex}}(P)}{2} \mp \frac{1}{2}\sqrt{[\epsilon_{\mathrm{ph}}(P) - \epsilon_{\mathrm{ex}}(P)]^2 + 4|\hbar\Omega_R|^2}. \tag{B3}$$

We note that $|X_P|^2$ and $|C_P|^2 = 1 - |X_P|^2$ represent the exciton and cavity photon fractions in the lower polariton, correspondingly.

[1] A. Kavokin and G. Malpeuch, *Cavity Polaritons* (Elsevier, Amsterdam, 2003).

[2] *Physics of Semiconductor Microcavities*, edited by B. Deveaud, special issue of Phys. Status Solidi B **242**, 1 (2005).

[3] P. Littlewood, Science **316**, 989 (2007).

[4] D. W. Snoke, *Solid State Physics. Essential Concepts* (Addison-Wesley, Boston, 2008).

[5] A. H. Castro Neto, F. Guinea, N. M. R. Peres, K. S. Novoselov, and A. K. Geim, Rev. Mod. Phys. **81**, 109 (2009).

[6] S. Das Sarma, S. Adam, E. H. Hwang, and E. Rossi, Rev. Mod. Phys. **83**, 407 (2011).

[7] A. Iyengar, J. Wang, H. A. Fertig, and L. Brey, Phys. Rev. B **75**, 125430 (2007).

[8] D. A. Abanin, A. V. Shytov, and L. S. Levitov, Phys. Rev. Lett. **105**, 086802 (2010).

[9] K. F. Mak, J. Shan, and T. F. Heinz, Phys. Rev. Lett. **106**, 046401 (2011).

[10] Yu. E. Lozovik and A. A. Sokolik, JETP Lett. **87**, 55 (2008).

[11] C.-H. Zhang and Y. N. Joglekar, Phys. Rev. B **77**, 233405 (2008).

[12] H. Min, R. Bistritzer, J.-J. Su, and A. H. MacDonald, Phys. Rev. B **78**, 121401(R) (2008).

[13] R. Bistritzer and A. H. MacDonald, Phys. Rev. Lett. **101**, 256406 (2008).

[14] M. Yu. Kharitonov and K. B. Efetov, Phys. Rev. B **78**, 241401(R) (2008).

[15] L. Yang, M. L. Cohen, and S. G. Louie, Nano Lett. **7**, 3112 (2007).

[16] L. Yang, M. L. Cohen, and S. G. Louie, Phys. Rev. Lett. **101**, 186401 (2008).

[17] L. Yang, J. Deslippe, C.-H. Park, M. L. Cohen, and S. G. Louie, Phys. Rev. Lett. **103**, 186802 (2009).

[18] Y. Zhang, T.-T. Tang, C. Girit, Z. Hao, M. C. Martin, A. Zettl, M. F. Crommie, Y. Shen, and F. Wang, Nature (London) **459**, 820 (2009).

[19] C.-H. Park and S. G. Louie, Nano Lett. **10**, 426 (2010).

[20] D. Haberer, D. V. Vyalikh, S. Taioli, B. Dora, M. Farjam, J. Fink, D. Marchenko, T. Pichler, K. Ziegler, S. Simonucci, M. S. Dresselhaus, M. Knupfer, B. Büchner, and A. Grüneis, Nano Lett. **10**, 3360 (2010).

[21] O. L. Berman, R. Ya. Kezerashvili, and K. Ziegler, Phys. Rev. B **85**, 035418 (2012).

[22] O. L. Berman, R. Ya. Kezerashvili, and Yu. E. Lozovik, Phys. Rev. B **80**, 115302 (2009).

[23] I. V. Lerner and Yu. E. Lozovik, Sov. Phys. JETP **51**, 588 (1980); **53**, 763 (1981); A. B. Dzyubenko and Yu. E. Lozovik, J. Phys. A **24**, 415 (1991).

[24] S. Pau, G. Björk, J. Jacobson, H. Cao, and Y. Yamamoto, Phys. Rev. B **51**, 14437 (1995).

[25] C. Ciuti, P. Schwendimann, and A. Quattropani, Semicond. Sci. Technol. **18**, S279 (2003).

[26] V. Lukose, R. Shankar, and G. Baskaran, Phys. Rev. Lett. **98**, 116802 (2007).

[27] V. Negoita, D. W. Snoke, and K. Eberl, Phys. Rev. B **60**, 2661 (1999).

[28] C. Ciuti, V. Savona, C. Piermarocchi, A. Quattropani, and P. Schwendimann, Phys. Rev. B **58**, 7926 (1998).

[29] S. Ben-Tabou de-Leon and B. Laikhtman, Phys. Rev. B **63**, 125306 (2001).

[30] G. Rochat, C. Ciuti, V. Savona, C. Piermarocchi, A. Quattropani, and P. Schwendimann, Phys. Rev. B **61**, 13856 (2000).

[31] B. Laikhtman, Europhys. Lett. **43**, 53 (1998).

[32] Le Si Dang, D. Heger, R. André, F. Boeuf, and R. Romestain, Phys. Rev. Lett. **81**, 3920 (1997).

[33] J. Kasprzak, M. Richard, S. Kundermann, A. Baas, P. Jeambrun, J. M. J. Keeling, F. M. Marchetti, M. H. Szymanska, R. André, J. L. Staehli, V. Savona, P. B. Littlewood, B. Deveaud, and Le Si Dang, Nature (London) **443**, 409 (2006).

[34] P. Kelkar, V. Kozlov, A. Nurmikko, C. Chu, J. Han, and R. Gunshor, Phys. Rev. B **56**, 7564 (1997).

[35] A. Kavokin and B. Gil, Appl. Phys. Lett. **72**, 2880 (1998).

[36] D. G. Lidzey, D. D. C. Bradley, T. Virgili, A. Armitage, M. S. Skolnick, and S. Walker, Phys. Rev. Lett. **82**, 3316 (1999).

[37] F. Manni, K. G. Lagoudakis, T. C. H. Liew, R. André, and B. Deveaud-Plédran, Phys. Rev. Lett. **107**, 106401 (2011).

[38] H. Deng, G. Weihs, C. Santori, J. Bloch, and Y. Yamamoto, Science **298**, 199 (2002).

[39] S. Christopoulos, G. Baldassarri Höger von Högersthal, A. Grundy, P. G. Lagoudakis, A. V. Kavokin, J. J. Baumberg, G. Christmann, R. Butté, E. Feltin, J.-F. Carlin, and N. Grandjean, Phys. Rev. Lett. **98**, 126405 (2007).

[40] M. Nakayama, Y. Kanatanai, T. Kawase, and D. Kim, Phys. Rev. B **85**, 205320 (2012).

[41] M. Zamfirescu, A. Kavokin, B. Gil, G. Malpuech, and M. Kaliteevski, Phys. Rev. B **65**, 161205(R) (2002).

[42] G. Christmann, R. Butté, E. Feltin, J.-F. Carlin, and N. Grandjean, Appl. Phys. Lett. **93**, 051102 (2008).

[43] D. Labilloy, H. Benisty, C. Weisbuch, T. F. Krauss, C. J. M. Smith, R. Houdré, and U. Oesterle, Appl. Phys. Lett. **73**, 1314 (1998).

[44] A. A. Abrikosov, L. P. Gorkov, and I. E. Dzyaloshinski, *Methods of Quantum Field Theory in Statistical Physics* (Prentice-Hall, Englewood Cliffs, NJ, 1963).

[45] A. Griffin, *Excitations in a Bose-Condensed Liquid* (Cambridge University Press, Cambridge, England, 1993).

[46] J. M. Kosterlitz and D. J. Thouless, J. Phys. C **6**, 1181 (1973); D. R. Nelson and J. M. Kosterlitz, Phys. Rev. Lett. **39**, 1201 (1977).